# Limiting electrical response of conductive and dielectric systems, stretched-exponential behavior, and discrimination between fitting models

J. Ross Macdonald[a)]
*Department of Physics and Astronomy, University of North Carolina, Chapel Hill, North Carolina 27599-3255*

Given a fitting model, such as the Kohlrausch–Williams–Watts (KWW)/stretched-exponential response, three plausible approaches to fitting small-signal frequency or time-response data are described and compared. Fitting can be carried out with either of two conductive-system formalisms or with a dielectric-system one. Methods are discussed and illustrated for deciding which of the three approaches is most pertinent for a given data set. Limiting low- and high-frequency log–log slopes for each of the four immittance levels are presented for several common models; cutoff effects are considered; and an anomaly in the approach to a single-relaxation-time Debye response for one of the conductive-system approaches is identified and explained. It is found that the temporal response function for the most appropriate conductive-system dispersion (CSD) approach, designated the CSD1, one long used in approximate form for frequency-response data analysis, does not lead to stretched-exponential transient behavior when a KWW response model is considered. Frequency-domain fitting methods and approaches are illustrated and discriminated using 321 and 380 K $Na_2O–3SiO_2$ data sets. The CSD1 approach using a KWW model is found to be most appropriate for fitting these data exceedingly closely with a complex nonlinear least-squares procedure available in the free computer program LEVM. Detailed examination and simulation of the approximate, long-used CSD1 modulus fitting formalism shows the unfortunate results of its failure to include separately the effects of the always present high-frequency-limiting dielectric constant, $\epsilon_{D\infty}$. The stretched-exponential exponent, $\beta$, associated with this fitting approach has always been misidentified in the past, and even after its reinterpretation, the result is likely to be sufficiently approximate that most physical conclusions derived from such fitting will need reevaluation. © *1997 American Institute of Physics.* [S0021-8979(97)00620-8]

## I. INTRODUCTION AND BACKGROUND

There are three different approaches to fitting and analyzing small-signal frequency and transient-response data for solid and liquid materials.[1–5] These involve fitting the data with either a complex dielectric constant, $\epsilon$, or susceptibility response model, appropriate for dielectric system dispersion (DSD), or with one of two different conductive-system-dispersion (CSD) approaches: CSD0 and CSD1, ones where the fitting model is defined at the complex resistivity, $\rho$, or impedance, $Z$, level. For such CSD situations, the limiting low-frequency conductivity or resistivity is an intrinsic part of the dispersive response model, not the case for the DSD situation. It is often convenient to express the models in terms of a distribution of relaxation times (DRT) or activation energies, but doing so, while mathematically useful, need not imply that such relaxation times, either continuously or discretely distributed, are necessarily of physical significance.

Any appropriate model or response function may be fitted to data using any of the three approaches described above. A crucial part of adequate fitting is to determine which of the three is most appropriate for a given set of experimental data and which available model best represents the data. Only then can the model and its parameter estimates lead to the physical insight and understanding that is the primary goal of experimentation.

The two different CSD approaches, ones with which we shall be most concerned here, are labeled CSD0 and CSD1. The CSD1 formalism is, from physical grounds,[3,5,6] particularly appropriate for thermally activated systems, but both will be considered and their responses compared here. Where needed, let us use a subscript $D$ to denote DSD-related quantities and $C$, 0, or 1 for the CSD ones. Thus, the DSD and CSD relaxation-time distributions may be designated as $G_D$, $G_0$, and $G_1$, respectively. Now, define an un-normalized frequency response quantity as $U_n$, where $n$ is $D$, 0, or 1. Thus, for example, $U_1$ might be a complex resistivity and $U_D$ a complex dielectric constant. Then, on defining $x \equiv \tau/\tau_{0n}$, where $\tau_{0n}$ is a characteristic relaxation time, one may write[3,5]

$$\frac{U_n(\omega)-U_n(\infty)}{U_n(0)-U_n(\infty)} \equiv I_n(\omega) = \int_0^\infty \frac{G_n(x)dx}{[1+i(\omega\tau_{0n})x]}. \tag{1}$$

Here, the $G_n$ quantities are taken normalized, so the normalized response quantity $I_n(\omega)$ satisfies $I_n(0)=1$ and $I_n(\infty)=0$.

It is worth emphasizing that although the $I_D$ response may be defined in terms of a distribution of dielectric-system dielectric relaxation times (Maxwell connectivity[7]) and the $I_C$ response in terms of a distribution of conductive-system resistivity relaxation times (Voigt connectivity[7]), their actual

[a)]Electronic mail: macd@gibbs.oit.unc.edu

frequency response can be fitted, for better or worse, by transformation of the data and model to any of the four immittance levels: complex dielectric constant, $\epsilon$; complex conductivity, $\sigma$; complex resistivity, $\rho$; and complex modulus, $M$. In terms of the normalized relaxation-time variable, $x$, the moments of the distributions may be expressed as[3,5]

$$\langle x^m \rangle_n \equiv \int_0^\infty x^m G_n(x)dx, \qquad (2)$$

where the $\langle x^m \rangle_n$ clearly depend on the shape of the distribution but not directly on $\tau_{0n}$. For simplicity, define $\rho_0'(0) \equiv \rho_{00}$ and $\rho_1'(0) \equiv \rho_{01}$. We shall usually omit this distinction and use just $\rho_0 = 1/\sigma_0$ instead.

A typical $I_n(\omega)$ response function is that of Havriliak and Negami,[8]

$$I_{HNn}(\omega) = [1 + (i\omega\tau_{0n})^{\alpha_n}]^{-\beta_n}, \quad 0 < \alpha_n \leqslant 1, \quad 0 < \beta_n \leqslant 1, \qquad (3)$$

an expression which reduces to the Cole–Cole[9] dielectric response when $n = D$ and $\beta_D = 1$, and to the Cole–Davidson[10] dielectric response when $\alpha_D = 1$. It has been shown[11] that any specific $I_D$ response function can be used at the CSD level with its parameters then designated by the subscript $C$ rather than $D$. Such changes are necessary since, although the form is the same, as one might expect, fitting of a given data set will not yield the same parameter estimates using the DSD fitting as those obtained with the CSD fitting.

The transformation from a DSD or CSD0 response function to a CSD1 one is somewhat more complicated. A limited and incorrect form of the needed relation was first proposed by Moynihan and co-workers;[6] a correct version was independently introduced later;[11] and the matter has been considered in detail recently.[3,5] The important and widely used Moynihan CSD1 data-fitting approach has been called the (Moynihan) modulus formalism (MMF),[5,12–14] because it was first derived and presented at the complex modulus level,[6] but it may be expressed at any immittance level. Given an expression for $I_0(\omega)$, a normalized complex resistivity (or impedance) quantity, the earlier work[3,5] shows that one can calculate $I_1(\omega)$ by

$$I_1(\omega) = [\langle x^{-1} \rangle_1 / i\omega\tau_{01}][1 - I_0(\omega)]. \qquad (4)$$

In the special case where $\rho_{C\infty} \equiv \rho_{C1}'(\infty) = 0$, that implicitly considered by Moynihan and co-workers, it turns out that if we define $M_1(\omega)$ in standard form as $(i\omega\epsilon_V\rho_{01})I_1(\omega)$, then

$$M_1(\omega) = [1 - I_0(\omega)]/(\epsilon_{C\infty})_1. \qquad (5)$$

Here, $\epsilon_V$ is the permittivity of vacuum. The quantity $(\epsilon_{C\infty})_1$, a purely conductive-system quantity, which is defined later in Eq. (7), was erroneously identified as one of the quite different quantities, $\epsilon_{D\infty}$ or $\epsilon_\infty$, by Moynihan and subsequent users of the modulus formalism.[6,12–14] It is particularly important to note that although a model expression for $I_0(\omega)$ may originally involve a shape parameter such as $\beta_0$, the corresponding $\beta_1$ associated with $I_1(\omega)$ through Eq. (4) will be unequal to $\beta_0$, a matter discussed in more detail below, because the distinction is both important and not generally understood.

Equations (4) and (5) were derived using the $G_n$'s of Eq. (1) and, in fact,[3,5] $G_1$ is proportional to $\tau$ (or $x$) times $G_0$. Note, however, that when an expression for $I_0(\omega)$ is available, $I_1(\omega)$ is readily obtained from Eq. (4) without the need for using $G_1$ in Eq. (1), provided an expression for $\langle x^{-1} \rangle_1$ is available, as it is for the important and much used Kohlrausch–Williams–Watts (KWW)[15] model. Conversely, when an analytic expression for $G_1$ is known but not one for $I_1(\omega)$, Eq. (1) may be used to obtain the latter. Further, the normalized temporal relaxation function, $\phi_n(t)$, is given by[3,16,17]

$$\phi_n(t) = \int_0^\infty G_n(\tau)\exp(-t/\tau)d\tau = \exp[-(t/\tau_{0n})^{\beta_n}],$$

$$0 < \beta_n \leqslant 1, \qquad (6)$$

where the right-hand side is the stretched-exponential (SE) response and only the $n = D$ or 0 choice is applicable for it, as demonstrated in the next section. When $n = D$, $\phi_D(t)$ gives the time dependence of the normalized charge measured on discharge of a completely charged purely dielectric material when its electrodes are shorted together. The interpretation of $\phi_n(t)$ for $n \neq D$ is more complicated, but the function is still useful and has been termed the correlation function by Ngai and Rizos[14] in such cases.

Although $I_n(\omega)$ may be calculated numerically from a known KWW $\phi_n(t)$ expression,[3,5,6,16,17] no closed-form KWW expressions for $I_n(\omega)$ are available when $\beta_n < 1$. Since, however, closed-form expressions for $G_0(\tau)$ and $G_1(\tau)$ are known[3,15,16] for $\beta_C = 0.5$, the left part of Eq. (6) may be used to obtain the $\phi_1(t)$ response for this particular KWW case. Since the MMF fitting approach has been primarily applied using the KWW response model for CSD situations, we shall here use the designation MMF only to indicate such fitting.

## II. TEMPORAL RESPONSE FUNCTIONS

Before discussing frequency response and fitting for CSD and DSD situations, it is useful to consider the corresponding transient or correlation-function response. Although the differences between the various responses could be illustrated, for example, for the Cole–Davidson response model, it is of greater interest to consider them for the KWW model, one which has been found to fit a large variety of experimental frequency-response data involving electrical or mechanical dispersion. Even though the present analysis deals explicitly with electrical behavior, its results apply as well to most mechanical relaxation situations.

Pertinent time-dependence results are presented in Fig. 1 for the $\beta_0 = 0.5$ case. The solid line shows an ordinary CSD0 or DSD stretched-exponential response for this value of $\beta_0 = \beta_D$. The solid line with solid circular points shows the corresponding CSD1 $\phi_1(t)$ response, calculated from the left-hand part of Eq. (6) using the KWW expression[3] for $G_1(\tau)$ with $\beta = \beta_1 = 0.5$ and the value of $\tau_s \equiv \tau_{o1}$ shown in Fig. 1. These results are expected to be accurate to one part in $10^6$ or better. Such high accuracy is only important because it ensures that when the model is used to fit experimental data, there[5] is no misfit contribution arising from in-
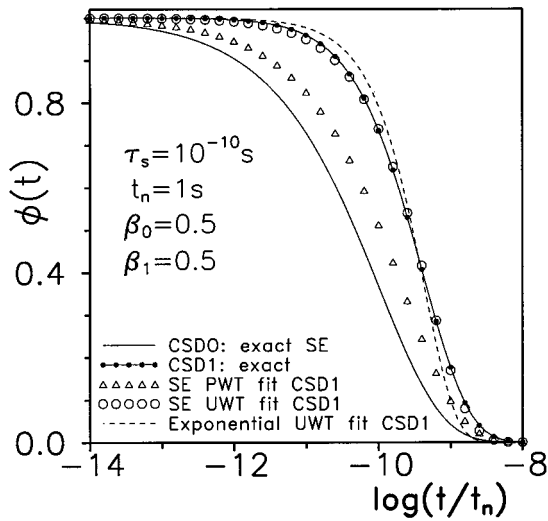
FIG. 1. Time dependence of the relaxation response function, $\phi(t)$, for two methods of calculating conductive-system response: (a) conventional stretched-exponential CSD0 behavior, and (b) the exact CSD1 response derived from modification of the conventional KWW distribution of relaxation times. Also shown are inadequate nonlinear least-squares fits to the (b) results using stretched- and ordinary-exponential-response models with proportional weighting (PWT) and unity weighting (UWT). Here $\tau_s = \tau_{on}$.

accurate model calculation, a source of ambiguity often present in prior frequency-response fitting using the KWW model.

Note that the CSD1 curve is not of stretched-exponential form. In previous work, not only has no theoretical CSD1 temporal response been presented for any model, but usually no distinction has been made between the various $\phi_n(t)$ responses.

The multiplication of $G_0$ by $\tau$ to obtain $G_1$, as discussed in the previous section, causes $G_1$ to approach zero faster than $G_0$ as $\tau \to 0$; it is, thus, narrower over the $\tau$ range. This, in turn, causes both the CSD1 temporal and frequency responses to be closer to those for the single-relaxation-time Debye response. Figure 2 shows such an approach in the frequency domain by means of complex-plane plots of CSD0, CSD1, and Debye $I_n(\omega)$ responses. Figure 1 includes the results of three weighted nonlinear least-squares fits to the CSD1 synthetic temporal data using the LEVM fitting program.[3,6,18] The first two fits used the SE model with either
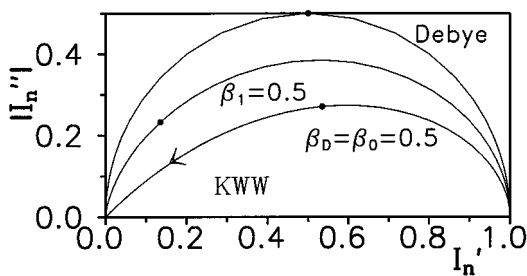


FIG. 2. Complex-plane comparisons of KWW DSD ($n=D$, $\beta_D = 0.5$), CSD0 ($n=0$, $\beta_0 = 0.5$), CSD1 ($n=1$, $\beta_1 = 0.5$), and Debye ($\beta=1$) normalized $I_n(\omega)$, responses. The solid dots show the positions where $\omega\tau_{on}=1$, and the arrow indicates the direction of increasing frequency for all the curves.

proportional weighting, where the weighting uncertainties are taken proportional to the data, or with unity weighting, i.e., no weighting, a choice which determines the fit primarily from the larger parts of the data. A logarithmic plot shows that the proportional-weighting results are much closer to the data for the $\phi(t) \ll 1$ region and that the unity-weighting ones are very poor in this region.

The proportional and unity-weighting SE fit estimates found for $\tau_s$ and $\beta$ were $2.1 \times 10^{-10}$ and $4.7 \times 10^{-10}$ s, and 0.54 and 0.77, respectively. If the CSD1 response were actually of the SE form, these results would be the same and independent of weighting. Thus, in spite of the apparently good unity-weighting SE fit shown in Fig. 1, the CSD1 temporal response associated with the KWW CSD0 response is not of SE form for $\beta_1 < 1$, and it seems unlikely that it can be expressed exactly in useful closed form for any $\beta$ value less than unity. Without such an expression, it is not possible to directly associate a plausible value of $\beta_1$ with the measured KWW CSD1 temporal response. For such response, the above results also show that for the SE-fit $\beta_1$ estimates, the relation $\beta_1 \simeq 1 - \beta_0$ does not hold, unlike the frequency-response situation discussed in the next section. For situations where the DRT is known for any $\beta_0$ value, such as that of the Cole–Davidson model, the value of $\beta_0$ used in calculating a $G_1$ for use in Eq. (6) may be used to label the resulting $\phi_1(t)$ response so long as it is not confused with a SE $\beta_1$ exponent-type parameter and is properly distinguished from the $\phi_0(t)$ response involving $\beta_0$.

It is worth mentioning that even for the KWW model, where no expression for $G_1$ is available for arbitrary $\beta_1$, but one can numerically calculate $I_1(\omega)$ accurately, as in the present work using LEVM, one can calculate the corresponding $\phi_1(t)$ by Fourier sine or cosine transformation of the real or imaginary part of $I_1(\omega)/\omega$.[16] For the KWW situation, we expect $\phi_1(t)$ to approach the single-exponential response as $\beta_1 \to 1$, but the calculation method outlined here, one which is prone to error, might nevertheless be worthwhile in order to investigate the non-SE CSD1 response expected, particularly that for the $\beta_1 < 0.5$ region.

Most empirical response functions, such as the Havriliak–Negami one, and many theoretical ones as well, are nonphysical.[19] In the frequency domain, the Cole–Cole response is nonphysical in both its low- and high-frequency limits, while the Cole–Davidson and KWW responses are nonphysical only in the high-frequency limit, where they predict a continuously increasing real-part conductivity. A reasonable way to restore physical realizability is to cut off the associated DRT at its ends;[3,19,20] only cutoff in the small-$\tau$ region, say at $\tau = \tau_{co}$, is needed for the Cole–Davidson and KWW response models. Such cutoffs are consistent with the requirement that any physically realizable process must have both a shortest nonzero response time and a longest noninfinite one as well.[19]

For $\tau$'s below cutoff, the response is dominated by the nonzero part of the DRT just before cutoff. The resulting response, either short-time temporal or high frequency, then approaches that of the response associated with a single (minimum) limiting relaxation time. For the KWW transient response, it follows that $\phi_n(t)$ must approach simple expo-

TABLE I. Limiting log–log slopes for CSD1, CSD0, and DSD situations. Results are applicable for either $\epsilon_{D\infty}=0$ or $\epsilon_{D\infty}\neq0$, except where the $\epsilon_{D\infty}=0$ ones (enclosed in square brackets) are included. For the CSD results, $\rho_{C\infty}=0$. LF and HF denote low- and high-frequency limits.

| Complex data/fit levels: | | | $\rho$ | $M$ | $\epsilon$ | $\sigma$ |
|---|---|---|---|---|---|---|
| CSD1 | LF | REAL | 0 | 2 | 0 | 0 |
| | | IMAG | 1 | 1 | $-1$ | 1 |
| | HF | REAL | $-(1+\beta_1)$ | 0 | 0 | $(1-\beta_1)$ |
| | | IMAG | $-1$ | $-\beta_1$ | $-\beta_1$ | 1 |
| CSD0 | LF | REAL | 0 | 2 | 0 | 0 |
| | | IMAG | 1 | 1 | $-1$ | 1 |
| | HF | REAL | $-(2-\beta_0)$ | 0 | 0 | $\beta_0$ |
| | | | $[-\beta_0]$ | $[1-\beta_0]$ | $[-(1-\beta_0)]$ | $[\beta_0]$ |
| | | IMAG | $-1$ | $-(1-\beta_0)$ | $-(1-\beta_0)$ | 1 |
| | | | $[-\beta_0]$ | $[1-\beta_0]$ | $[-(1-\beta_0)]$ | $[\beta_0]$ |
| DSD ($\sigma_0=0$) | LF | REAL | 0 | 0 | 0 | 2 |
| | | IMAG | $-1$ | 1 | 1 | 1 |
| | HF | REAL | $-(1+\beta_D)$ | 0 | 0 | $1-\beta_D$ |
| | | | $[-(1-\beta_D)]$ | $[\beta_D]$ | $[-\beta_D]$ | $[1-\beta_D]$ |
| | | IMAG | $-1$ | $-\beta_D$ | $-\beta_D$ | 1 |
| | | | $[-(1-\beta_D)]$ | $[\beta_D]$ | $[-\beta_D]$ | $[1-\beta_D]$ |
| DSD ($\sigma_0\neq0$) | LF | REAL | 0 | 2 | 0 | 0 |
| | | IMAG | 1 | 1 | $-1$ | 1 |
| | HF | REAL | $-(1+\beta_D)$ | 0 | 0 | $1-\beta_D$ |
| | | | $[-(1-\beta_D)]$ | $[\beta_D]$ | $[-\beta_D]$ | $[1-\beta_D]$ |
| | | IMAG | $-1$ | $-\beta_D$ | $-\beta_D$ | 1 |
| | | | $[-(1-\beta_D)]$ | $[\beta_D]$ | $[-\beta_D]$ | $[1-\beta_D]$ |

nential behavior as $\tau$ becomes smaller than $\tau_{\mathrm{co}}$, a conclusion reached independently long ago by Ngai[21] for the $\phi_D(t)$ case. The results in Fig. 1 show that if such transformation happened for the present CSD1 response with $\tau_{\mathrm{co}} = 10^{-12}$ s, it would be very difficult to distinguish it from an ordinary $\phi_1(t)$ response without cutoff, although identification of cutoff effects is likely to be better in the frequency domain, as illustrated by the results shown in Ref. 22.

## III. LIMITING LOG–LOG SLOPES IN THE FREQUENCY DOMAIN

### A. General slope results

It proves to be instructive to compare the low- and high-frequency limiting log–log slopes of the frequency response of a single dispersive process at all four immittance levels. For simplicity, log–log slopes will be referred to hereafter just as slopes. In Table I, slope results are shown for response models, such as the Cole–Davidson, KWW, and Cole–Cole (with long-$\tau$ cutoff), which are intrinsically physically unrealizable in the high-frequency limit without any cutoff at a small $\tau$ value. We, thus, are able to show what these high-frequency limiting slopes are, and, in addition, as discussed below, their values with cutoff present may be directly obtained as well. For the exponential distribution of relaxation model with cutoff at both frequency extremes, some idealized graphical slope results appear in Ref. 23. The Table I results were verified by complex nonlinear least-squares (CNLS) fitting using the LEVM program.[18] Until recently, accurate and rapid calculation of the KWW CSD0 and CSD1 frequency response for data fitting was unavail-

able, but now a KWW addition to LEVM is available, one which yields accuracy of one part in $10^6$ or better.[5]

Note that the $\beta$ values in Table I repesent those of any of the above models, with the $\alpha$ of Eq. (3) here taken as $\beta$ for the Cole–Cole response and as 1 for the Cole–Davidson model. Although $\epsilon_{D\infty}$ is $>1$ for any real material, results are shown in Table I for $\epsilon_{D\infty}=0$ as well, in order to illustrate the tremendous differences in slopes between the two cases for some situations. These differences are worth emphasizing because the standard way of fitting data at the CSD1 level to the KWW model using the MMF takes no separate account of $\epsilon_{D\infty}$. For the CSD results, $\rho_{C\infty}$ is taken as zero. For the DSD situations, where conductive-system dispersion is assumed absent, results are presented for both $\sigma_0\equiv\sigma'(0)=0$ (pure dielectric response) and for $\sigma_0\neq0$ (leaky dielectric response). The latter choice is necessary for a direct fitting comparison with the CSD response.

One might wonder why, since both the CSD0 and CSD1 response possibilities are considered in Table I, only DSD, rather than DSD0 and DSD1, behavior is included here. In terms of previous definitions, DSD is the same as DSD0, but a DSD1 formalism would only be appropriate[11] for situations where both $\Delta\epsilon_D\equiv\epsilon_{D0}-\epsilon_{D\infty}$ and $\tau_{oD}$ were thermally activated with the same or comparable activation energies, not the usual situation.

It is important to emphasize that the slopes presented in Table I in terms of the $\beta$ parameters of a fitting model involve the specific $\beta$'s of a given model. Thus, if, for a specific model, a set of exact simulated CSD1 data was calculated with a particular value of $\beta$, say $\beta_1$, and then fitted

J. Appl. Phys., Vol. 82, No. 8, 15 October 1997

J. Ross Macdonald    3965

using the CSD0 form of the model, the resulting estimate of $\beta$ would be designated $\beta_0$, not $\beta_1$. This procedure has been followed here, and Table I shows that, as far as limiting slopes are concerned, when $\epsilon_{D\infty}$ is $>0$, $\beta_0 = 1 - \beta_1$ (but see the $\beta_0 \to 1$ discussion below). For actual data, fits over the principal response range should not be expected to agree perfectly with this relation, even when both CSD0 and CSD1 fits are excellent, but one should expect it to be a good approximation provided the data range is adequate. Some such results are presented in the next section.

There is a lot of information in Table I. Note that when the low-frequency and high-frequency imaginary-part slopes are of opposite sign, there will be a peaked response between these regions. For the $\epsilon_{D\infty} \neq 0$ situation, there are two such response possibilities for each CSD or DSD set, with one of them always involving $M''$. Further, note the equivalence at each immittance level, when $\epsilon_{D\infty} \neq 0$ and $\beta_D = \beta_1$, between the CSD1 slopes and those for DSD when $\sigma_0 \neq 0$. Finally, compare the CSD0 results with $\epsilon_{D\infty} = 0$, with the DSD ones having both $\epsilon_{D\infty} = 0$ and $\sigma_0 = 0$, after the following shifts of the immittance level.[11] $\rho \leftrightarrow \epsilon$, and $M \leftrightarrow \sigma$. There is, then, full equivalence if one sets $\beta_D = \beta_0$. Note that the high-frequency CSD0 $\sigma'(\omega)$ slope of $\beta_0$ in Table I implies a response of the form $(\omega \tau_{o0})^{\beta_0}$ when $(\omega \tau_{o0}) \gg 1$.

A few results in Table I have been presented earlier for the KWW conductivity relaxation situation but with incomplete identification.[24] These are the CSD0 low- and high-frequency $\sigma'(\omega)$ and $\epsilon''(\omega)$ values appropriate when $\beta_0$ is taken as the SE value of $\beta_n$ in the right side of Eq. (6), and such a $\beta_0$ is frequently written[12,14,24] as $1 - n$ or $\beta$. Reference 24 was published before the distinction between the CSD0 and CSD1 approaches was fully recognized, and it actually deals with the MMF CSD1 frequency response, a response involving the CSD1, not CSD0, slopes listed in Table I.

The various similarities and equivalencies illustrated in Table I indicate that when $\epsilon_{D\infty} \neq 0$ one might be able to fit CSD1 data with either CSD0 or DSD (with $\sigma_0 \neq 0$) or *vice versa*. This suggests that in some cases, it may be difficult to decide which type of fitting is the more appropriate. See the illustration and discussion in Sec. IV.

## B. The transition to Debye response

A stretched-exponential response, as in the right-hand side of Eq. (6) for $\beta_n = \beta_0$ or $\beta_D$, leads to a simple-exponential response when these exponent quantities are unity. It is, thus, reasonable to expect that in this limit the associated frequency response should degenerate to a single-time-constant, nondispersed Debye response. In spite of the failure of the KWW1 temporal response to be of SE form for $\beta_1 < 1$, as discussed in Sec. II, the Debye frequency response does indeed appear for all three cases when the relevant $\beta$ is unity. But there is an apparent anomaly for the CSD0 situation. A characteristic of the pure conductive-system Debye response is that the $\sigma'$ slope is zero at all frequencies, apparently in direct contradiction to the $\sigma'$ high-frequency slope of $\beta_0$ listed in Table I for CSD0 behavior when $\beta_0 = 1$, and inconsistent as well with the relation $\beta_0 = 1 - \beta_1$ when $\beta_1 = 1$.

Suppose we consider a value of $\beta = 1 - \delta$, with $\delta \to 0$. The $\sigma$ column in Table I shows that one expects a limiting slope of $\delta$ for CSD1 and $1 - \delta$ for CSD0. These results are indeed found, but the smaller $\delta$, the higher the frequency required for the transition from the zero low-frequency slope to the limiting high-frequency slope to occur, and the final limiting CSD0 slope of unity only appears at infinite frequency. For example, for the KWW0 model as $\beta_0$ increases from 0.99 to 0.999 to 0.9999, the corresponding values of $(\omega_H \tau_{o0})$, the normalized frequency at which the actual $\sigma'(\omega)$ slope has increased from zero to $0.5\beta_0$, increases from approximately 64 to 640 to 6400.

These results suggest that one should be careful in interpreting the limiting high-frequency CSD0 response in the neighborhood of $\beta_0 = 1$. But the above anomaly actually never arises because in real systems low-$\tau$ cutoff is always present and leads to a limiting Debye response at a finite high frequency, independent of the value of $\beta$. Therefore, the actual high-frequency limiting slopes for all experimental data are those obtained on setting $\beta_D$ or $\beta_1$ to unity and $\beta_0$ to zero in Table I. Thus, cutoff induces a transition from the CSD0 slope value of $\beta_0$ to a plateau with zero slope.

## IV. FREQUENCY RESPONSE, FITTING, AND MODEL DISCRIMINATION

### A. CNLS fitting results

In recent work,[5] it has been found that for $Na_2O$–$3SiO_2$ frequency response data[25] extending over the temperature range from 303 to 398.5 K, the newly available accurate KWW computational models in LEVM indicate that the data are best fitted with the CSD1 approach. Let us designate such CSD1 KWW fitting by KWW1, that using CSD0 as KWW0, and DSD KWW fitting as KWWD. Here, further KWW fitting of the 321 K data set will first be presented to illustrate how one might discriminate between CSD1, CSD0, and DSD fitting when data at only a single temperature are available, and to compare such fitting results with those obtained by the MMF approach.

For simplicity, the data set was initially modified to eliminate, insofar as possible, electrode polarization effects. As demonstrated earlier,[5] LEVM is first used to fit the data to a composite model, which includes both KWW1 and the electrode-response parts. Then, LEVM is used to eliminate from the data the full effects of the fit estimate of the electrode contribution. Subsequent fitting of the pruned data set with the KWW1 model alone, then yields very nearly as good a fit as the original one, as well as essentially the same common parameter estimates. Here, only such modified data sets are considered, but one should always investigate the possibility that electrode polarization effects are non-negligible when fitting experimental CSD data.

It is usually clear whether to use CSD or DSD fitting of data when data sets at several temperatures are available. If no evidence of a $\rho_0$ is found, and the dispersed response is not thermally activated, then one is most likely dealing with a DSD situation. But if a $\rho_0$ appears to exist, and it and $\tau_0$ are thermally activated with at least approximately the same activation energies, then it is most likely that CSD is present,

TABLE II. Fitting results for (a) 321 K Na$_2$O–3SiO$_2$ data and (b) synthetic data generated from CSD1-a fit parameters. Top five rows are CNLS fits at complex-$M$ level; bottom five rows are (a)-type $M''$ fits. All fits involved proportional weighting (PWT or P) except those marked U for unity weighting (UWT). $\epsilon_{D\infty}$ is a free fitting parameter for all fits except the last three, where $N$ indicates that no such parameter is present. For CSD, $\epsilon_X = \epsilon_{C0}$, and for DSD, $\epsilon_X = \Delta\epsilon_D$. $S_F$ is the standard deviation of the fit relative residuals.

| Type: | $100S_F$ | $\beta_n$ | $10^{-9}\rho_{0N}$ | $10^4\tau_{nN}$ | $10^3\langle\tau_{nN}\rangle$ | $\epsilon_{D\infty}$ | $\epsilon_{C\infty}$ | $\epsilon_X$ | $\epsilon_\infty$ | $\epsilon_0$ |
|---|---|---|---|---|---|---|---|---|---|---|
| CSD1-a | 0.272 | 0.425 | 1.441 | 2.396 | 3.111 | 4.83 | 5.34 | 24.38 | 10.17 | 29.20 |
| CSD0-a | 0.570 | 0.543 | 1.439 | 13.32 | 2.314 | 10.21 | 0 | 18.17 | 10.21 | 28.37 |
| CSD0-b | 0.554 | 0.542 | 1.438 | 13.30 | 2.314 | 10.21 | 0 | 18.18 | 10.21 | 28.39 |
| DSD-a | 0.646 | 0.464 | 1.451 | 33.37 | 7.728 | 10.21 | ··· | 21.36 | 10.21 | 31.57 |
| DSD-b | 0.535 | 0.463 | 1.456 | 37.86 | 8.839 | 10.21 | ··· | 22.37 | 10.21 | 32.57 |
| CSD1-P | 0.352 | 0.426 | 1.448 | 2.474 | 3.151 | 4.73 | 5.44 | 24.58 | 10.17 | 29.30 |
| CSD1-U | 0.378 | 0.424 | 1.450 | 2.426 | 3.153 | 4.78 | 5.37 | 24.55 | 10.15 | 29.34 |
| CSD1-PN | 3.51 | 0.482 | 1.565 | 6.920 | 4.659 | ··· | 10.26 | 33.62 | 10.26 | 33.62 |
| CSD1-UN | 5.60 | 0.496 | 1.557 | 6.990 | 4.334 | ··· | 10.29 | 31.44 | 10.29 | 31.44 |
| CSD0-UN | 50.1 | 0.943 | 0.893 | 12.66 | 1.300 | ··· | 0 | 16.44 | 0 | 16.44 |

since any leakage $\rho_0$ apparent for a DSD situation is unlikely to be related to the dielectric dispersion process and, thus, it will not have the same or similar activation energy as the latter. But when data for only a single temperature are available, comparison of the CSD1 response with that for DSD (with $\epsilon_{D\infty}\neq 0$ and $\sigma_0\neq 0$) in Table I shows that they involve identical limiting behavior when $\beta_D = \beta_1$. Then, a more detailed fitting comparison is required in order to discriminate properly between the two cases.

A variety of LEVM fitting results for the 321 K data are presented in Table II. Here, $\rho_{0N}\equiv\rho_0/\rho_d$, where $\rho_d = 1\ \Omega$ cm, and $\tau_{nN}\equiv\tau_n/\tau_d$ with $\tau_d = 1$ s. As defined earlier, $\rho_0\equiv\rho_n'(0)$ and $n = 0, 1$, or $D$. Fitting was carried out at the complex $M$ level using Eqs. (1) and (4) along with a contribution from the fitting parameter $\epsilon_{D\infty}$ when it was taken as nonzero and free to vary. The parameter $\rho_{C\infty}$ was found to make no contribution to the fits and so was not included in the fittings. Although the KWW1-fit quantity $I_1(\omega)$ is here calculated using the $I_0(\omega)$ of Eq. (4), the original $\beta_0$ of the latter is renamed and reinterpreted as $\beta_1$ for the KWW1 fits. Finally, note that all full CNLS CSD fit results shown in Table II, which involve proportional weighting, yield the same results whether the fitting is carried out at the complex $\rho$ or complex $M$ level.[3–5] CNLS proportional-weighting fitting at the complex $\epsilon$ or complex $\sigma$ levels yielded results close to those for the $\rho$ or $M$ level. The DRT moment $\langle x^{-1}\rangle_1$ needed in the KWW1 fits is given by[3,5] $[(\langle x\rangle_0)_1]^{-1}$, where this notation indicates that the CSD0 (or DSD) form of the average, the one which involves the SE exponent and its associated DRT for KWW situations, is to be used but with $\beta_0$ changed to $\beta_1$. It follows that for the KWW1 model $\langle x^{-1}\rangle_1 = \beta_1/\Gamma(1/\beta_1)$, where $\Gamma$ is the gamma function. Note that for the $\beta$ estimates of lines 1 and 2, $\beta_1\simeq 1 - \beta_0$, as expected. A few KWW1 fits were carried out using Eq. (5), with $(\epsilon_{C\infty})_1$ a free parameter rather than $\rho$. When $\epsilon_{D\infty}$ was also included as a free parameter, exactly the same results as those shown in line 1 of Table II were then obtained, as expected.

The results for the standard deviation of the relative residuals of the fit, $S_F$, show that this quantity is appreciably smaller for the KWW1 fit of line 1 than that for the KWW0 fit of line 2, or the KWWD fit of line 4. This, and the exceptionally small value of the line-1 $S_F$, is a strong indication

that KWW1 fitting is most appropriate for these data. To explore this possibility further, the fitting parameters of the line-1 fit were used to generate exact KWW1 model data at the same frequencies as those of the original experimental data. The results of fitting this data set by the CSD0 and DSD approaches are shown in lines 3 and 5. Comparison with the results of lines 2 and 4 shows that the $S_F$ and parameter values are very little changed for the CSD0 case and only slightly more modified for the DSD one. These results thus indicate that the main differences between the estimates of lines 1, 2, and 4 are systematic, not random, and thus, they are associated with the use of the less appropriate, for these data, CSD0 and DSD fitting approaches.

For simplicity, the relative standard deviations of the fitting parameters themselves have been omitted from Table II, but they are very small for the line-1 KWW1 fit,[5] and they increase with increasing $S_F$. Further information about the KWW1, KWW0, and KWWD $M$-level fits is provided by the curves presented in Fig. 3 for the relative residuals of the imaginary (3-a) and real (3-b) parts. These results also apply to $\rho$-level fitting if the $r''$ and $r'$ labels are reversed. The increases in the residuals at the frequency extremes probably arise from inexact estimation of the electrode-polarization effects, errors which are magnified on subtraction. Measurements over a wider response range would allow better identification of the electrode effects and, thus, more accurate subtraction.

Note especially the similarity between the residuals arising from the KWWD fit of the experimental data and the KWWD fit of the exact CSD1 model data. If one uses the residuals for the line-1 KWW1 data fit to correct those of the line-4 KWWD data fit, the results are very close to those for the line-5 DSD fit to the KWW1 model data. In spite of the excellence of the line-1 KWW1 fit, the associated residuals show some small remaining serial correlation, nonrandomicity arising either from the measurement procedure or from a small systematic deviation in the KWW1-fit model from the actual experimental response.

The results in columns 2–7 of Table II are direct CNLS fitting estimates. Although the estimates marked $\epsilon_{D\infty}$ are actual $\epsilon_{D\infty}$ ones for the CSD1 and DSD fits, they are forced to be estimates of $\epsilon_\infty$ for the KWW0 fits of lines 2 and 3. Further, note the large differences between the 0.425 $\beta_1$ es-

J. Appl. Phys., Vol. 82, No. 8, 15 October 1997

J. Ross Macdonald   3967
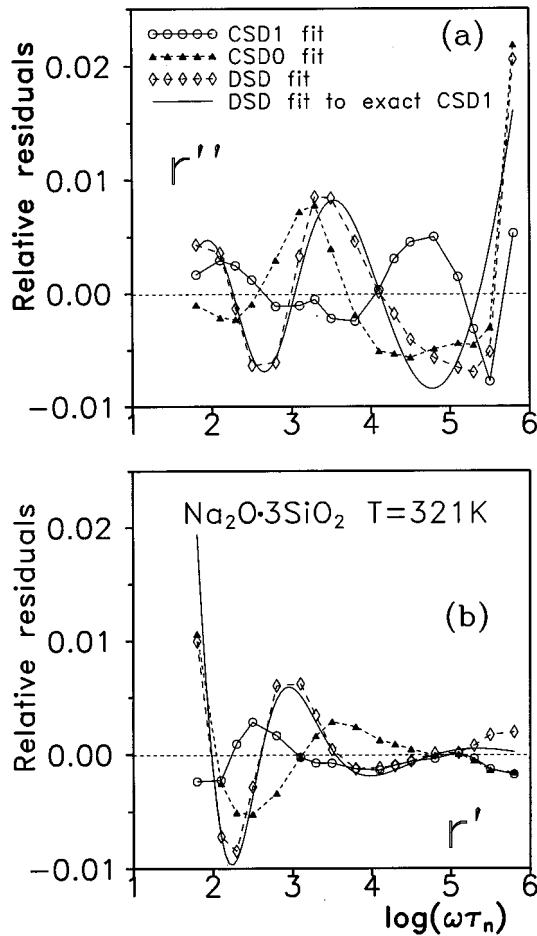
FIG. 3. Relative residuals for KWW CSD1, CSD0, and DSD complex nonlinear least-squares fits with proportional weighting to Na$_2$O–3SiO$_2$ frequency response data at 321 K (See Table II). For $M(\omega)$ fitting, the residuals are those associated with $M'(\omega)(3-b)$ and $M''(\omega)(3-a)$ as shown, but the identifications are reversed for fitting at the $\rho(\omega)$ level. Here and hereafter $\tau_n = 1$ s.

timate of line 1 and the KWW0 $\beta_0$ estimates of lines 2 and 3. If we repeat the line-1 fit without any free $\epsilon_{D\infty}$ parameter, the resulting $\beta_1$ estimate is 0.495, much closer to the $\beta_0$ ones, but $S_F$ is ten times larger. Further synthetic KWW1 data studies with $\epsilon_{D\infty}$ ranging from 5 to 45 indicated that for KWW0 fits including a free $\epsilon_{D\infty}$ parameter as in line 3, the $\beta_0$ estimates and $S_F$ values found were virtually independent of $\epsilon_{D\infty}$ over this range, but not including $\epsilon_{D\infty}=0$. On the other hand, KWW1 fits without any $\epsilon_{D\infty}$ led, as the $\epsilon_{D\infty}$ values in the data were increased, to larger and larger values of $S_F$ and to larger $\beta_1$ estimates, with the $\beta_1$ estimate reaching 0.6 by $\epsilon_{D\infty}=45$. These important findings are further explored in the context of conventional MMF fitting in the next section.

For the DSD results, the model does not, of course, include an $(\epsilon_{C\infty})_1$ CSD contribution, so DSD fitting is unable to discriminate between the $\epsilon_{D\infty}$ and $(\epsilon_{C\infty})_1$ contributions to $\epsilon_\infty$ involved in actual CSD1-type data, and so lumps them together. The present important results again underline the appropriateness of fitting thermally activated CSD-type data with the CSD1 approach, not with either the CSD0 or the DSD one.

For the last four columns in Table II, all quantities except the $\epsilon_X = \Delta\epsilon_D$ DSD estimates are calculated from the direct fitting results. For example, $\epsilon_\infty = (\epsilon_{C\infty})_1 + \epsilon_{D\infty}$, and $\epsilon_0 = \epsilon_X + \epsilon_{D\infty}$. The CSD1 quantities are given in general and for the KWW response by[3,5]

$$(\epsilon_{C\infty})_1 = \tau_{01}(\langle x\rangle_0)_1 / \epsilon_V\rho_0 = \tau_{01}\Gamma(1/\beta_1)/\beta_1\epsilon_V\rho_0, \quad (7)$$

and

$$(\epsilon_{C0})_1 = \tau_{01}\langle x\rangle_1 / \epsilon_V\rho_0 \equiv \langle\tau\rangle_1 / \epsilon_V\rho_0, \quad (8)$$

where[3] $\langle x\rangle_1 = (\langle x^2\rangle_0)_1 / (\langle x\rangle_0)_1$. For the KWW response, it follows that[16] $\langle x\rangle_1 = \Gamma(2/\beta_1)/\Gamma(1/\beta_1)$. For comparison with Eq. (7), the modern form of the CSD1 Moynihan modulus formalism expression is[5,13,14,26]

$$\epsilon_\infty = \tau_{01}\Gamma(1/\beta_0)/\beta_0\epsilon_V\rho_0. \quad (9)$$

Notice that not only does this result involve $\epsilon_\infty$ (which is never a pure CSD quantity) instead of $(\epsilon_{C\infty})_1$, but it also involves $\beta_0$ (written in the past as $\beta$ because the $\beta_1$, $\beta_0$ distinction has only recently been explicitly recognized[5]) rather than $\beta_1$ as in Eq. (7). As the results of Table I show, these quantities are quite different except when they are both 0.5. Equation (7) indicates that $(\epsilon_{C\infty})_1/(\langle x\rangle_0)_1$ and $(\epsilon_{C0})_1/\langle x\rangle_1$ must both be temperature independent in order for $\tau_{01}$ and $\rho_0$ to have exactly the same activation energy.

### B. $M''$ fitting results and the Moynihan modulus formalism

The last five rows in Table II involve nonlinear least-squares fitting of the imaginary-part $M''(\omega)$ experimental data to a KWW model in order to obtain results for comparison with those found using the MMF, a formalism which does not use CNLS fitting. The CSD1-P and CSD1-U results are both comparable to the CNLS ones of line 1. If the model is appropriate for the data, not only should the fits with the same weighting be closely comparable, as they are, but also the fit estimates should be very nearly independent of the weighting, just as we see here. These fits, thus, further strongly support the previous conclusion that the KWW1 fit model is the most appropriate one for these data.

The last three rows of Table II involve fits without any fitting parameter included to estimate $\epsilon_{D\infty}$, since the MMF takes no separate account of this quantity. The omission of this parameter clearly leads to far worse fits of the $M''(\omega)$ data than those obtained when it is included. Figure 4 presents the $M''(\omega)$ plots for these last three fits. Since the line-1 fit results are indistinguishable from the data points on a plot of this kind, they are omitted to reduce clutter in the graph. Figure 4 makes it clear why the CSD0 fit involves a $S_F$ value nearly 200 times larger than the line-1 one. Clearly, even though full KWW0 fitting with proportional weighting, as in line 2, can yield a good fit, the result for the $M''(\omega)$ fitting when unity weighting is used and $\epsilon_{D\infty}$ is omitted, is completely unacceptable.

The MMF approach[3,5,6,12] used an approximate inversion method to estimate discrete values of $G_0$ (denoted ''g'' in that work) and employed the results to calculate template curves of $I_0(\omega)$ and $\{1-I_0(\omega)\}$ for a variety of $\beta$ (here $\beta_0$) values. Equation (5) shows that $\{1-I_0(\omega)\}$ is a normalized
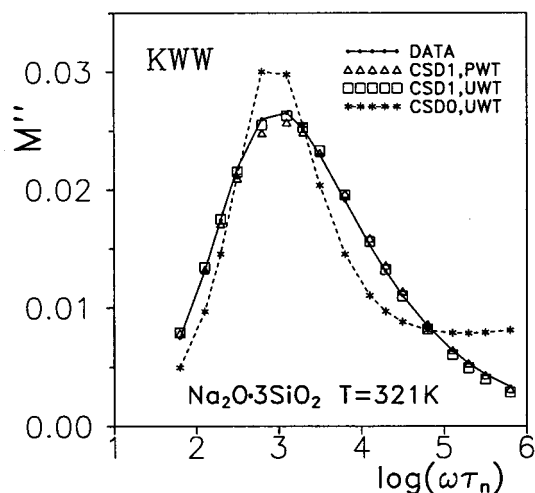
FIG. 4. Results of nonlinear least-squares KWW fitting of the 321 K, $Na_2O–3SiO_2$ $M''(\omega)$ data without taking separate account of the high-frequency limiting dielectric constant $\epsilon_{D\infty}$ (see the last three lines in Table II). The results of the CSD1 fit with unity weighting are most appropriate for comparison with the results of a conventional modulus-formalism fit of the same data.

form of $M_1(\omega)$, so in this and subsequent MMF fitting work, plots of the imaginary part (and sometimes the real part)[12] of $\{1 - I_0(\omega)\}$ were constructed and usually compared to $M''(\omega)$ data in order to estimate values of $\epsilon_{D\infty}$ (or $\epsilon_\infty$), $\beta$, and $\tau_0$ (here denoted $\tau_{01}$). Note that this procedure ignores the effect of a separate $\epsilon_{D\infty}$ parameter and emphasizes the large parts of $M''(\omega)$ at the expense of the smaller tail regions. This is just what the CSD1-UN fit in Table II does, so we may expect that it should yield results comparable to those obtained with the MMF.

The CSD1-PN and CSD1-UN lines in Table II show $\beta_1$ estimates that are much larger than that of the best-fit result of line 1. The CSD1-UN fit involves a rounded value of 0.50. Further, a CSD1-UN fit using Eq. (5) instead of Eq. (4) yields exactly the same results, confirming that the corrected MMF approach can yield results consistent with the usual KWW1 one generally employed here. It has been stated[27] that ''large electrode capacitances... need not interfere with the analysis of relaxation phenomena when the data are analyzed using the electrical modulus formalism...'' Earlier work[3–5] has shown, however, that electrode-polarization effects should not be neglected. Further, comparison of the CSD1-P and CSD1-U results in Table II, ones that include the presence of $\epsilon_{D\infty}$, whose capacitance effects are generally much smaller than electrode ones, with the CSD1-PN and CSD1-UN ones, shows that neglecting $\epsilon_{D\infty}$ for these last two fits has strongly deleterious consequences both for the goodness of fit of the data and for the parameter estimates themselves.

## C. Temperature dependence of $\beta$'s and their proper identification

It should now be clear that although all published MMF CSD1 fits erroneously identified their $\beta$ estimates with those of the corresponding SE temporal response, $\beta_0$ in the present

analysis, the actual $\beta$'s, derived directly from CSD1 frequency response fits, should be identified with $\beta_1$. Let us designate them as $\beta_{1MMF}$, a different quantity than the KWW1-fit estimates of $\beta_1$, which take proper account of $\epsilon_{D\infty}$. When the relation $\beta_1 = 1 - \beta_0$ holds and $\beta_1 = 0.5$, as above for the CSD1-UN $T = 321$ K data fit, the $\beta$'s are numerically identical, blurring the distinction between them. Now, it luckily turns out that the present $Na_2O–3SiO_2$ data sets were fitted by the MMF approach at the Naval Research Laboratory, and the results are listed in Ref. 25. The $\beta_{1MMF}$ and $\tau_{01}$ values quoted there are, for example, 0.50 and 0.53 and $8.0 \times 10^{-4}$ s and $1.6 \times 10^{-5}$ s for the 321 and 380 K data fits, respectively.

Because of the ambiguity of the $\beta_{1MMF} = 0.5$ value, it is worthwhile to include here the results of data fits at another temperature where $\beta_{1MMF} \neq 0.5$. Although the 380 K data do not extend to high enough frequencies to yield much of the high-frequency part of the $M''(\omega)$ curve beyond its peak, enough is present to yield adequate KWW1 fits. Similarly to the 321 K data, electrode polarization effects were subtracted from the data[5] before the present fits were carried out. The following $\beta_1$ estimates were obtained: (a) CNLS $M(\omega)$ fitting including $\epsilon_{D\infty}$ and with no $\epsilon_{D\infty}$ [ ]: CSD1-P, 0.36, [0.53]; and CSD1-U, 0.37, [0.54]. (b) $M''(\omega)$ fitting: CSD1-P, 0.41, [0.53]; and CSD1-U, 0.40, [0.53]. Again, the large effect of including or omitting $\epsilon_{D\infty}$ is evident both for CNLS and for NLS fitting. In addition, the relation $\beta_1 = 1 - \beta_0$ holds less well, as expected, for these higher temperature results than for the 321 K ones.

The above 321 and 380 K unity-weighting fit results with no separate account of $\epsilon_{D\infty}$ are consistent in yielding $\beta_1 \simeq 0.50$ and 0.53, respectively, quite different from the estimates obtained when $\epsilon_{D\infty}$ is properly included, but the same as those found in the Naval Research Laboratory MMF fits. Further, the present unity-weighting fits without $\epsilon_{D\infty}$ led to estimates of about $7.0 \times 10^{-4}$ s and $1.58 \times 10^{-5}$ s, close to the Naval Research Laboratory one for 321 K and very close to the 380 K one. Such agreement indicates that the present method of approximating MMF fitting is quite adequate.

These results indicate that CNLS fitting is more appropriate than the NLS fitting, that the CSD fitting should not be carried out without including the $\epsilon_{D\infty}$ effects, and, most important, that all previous MMF-fit estimates of $\beta_1$, which were identified with $\beta_0$ but here are designated as $\beta_{1MMF}$, should be recalculated as $1 - \beta_{1MMF}$ and then identified as approximate $\beta_1$ values.

The above renaming and reevaluation should usually allow previously published MMF $\beta$ values to be brought closer to those actually appropriate for CSD data, but, as shown by the present results, such changes only go part way toward obtaining proper KWW1 estimates. In previous work,[5] I compared CNLS KWW1 proportional-weighting-fit estimates, including $\epsilon_{D\infty}$, of $\beta(=\beta_1)$ with those obtained by the Naval Research Laboratory MMF fits and showed that the latter exhibited an *opposite* temperature response over the range from 303 to 398.5 K to that of the KWW1 fits. Unfortunately, at that time I did not know enough to properly identify the Naval Research Laboratory estimates as done above. The bottom curve in Fig. 6 of Ref. 5 is one for $\beta_1$

versus 1000/T, and the top Naval Research Laboratory curve, when replaced by $1 - \beta_{1MMF} \sim \beta_1$, is closer to the bottom curve, no longer shows opposite temperature dependence, but still lies appreciably above the bottom one.

There is not a large amount of CSD KWW $\beta$ versus temperature data available in the literature, nor plausible theory available for interpreting its temperature dependence. The available results generally indicate that $\beta$ is either constant over a limited temperature range or often shows a general tendency to increase, probably toward unity and a Debye response, as the temperature increases,[25,28] but the behavior can be more complicated near the glass transition, and a decrease in $\beta$ with increasing temperature has been found in the liquid region of a glass-forming molten salt.[29] An increase of $\beta_0$ with increasing temperature implies that the proper CSD1 $\beta_1$ will decrease with temperature increase.[5] Finally, Angell[30] has drawn attention to results where the temperature dependence of $\beta$ from electrical measurements on a material was opposite to that obtained for shear relaxation processes. It is worth considering whether any such discrepancies can be explained by the improper use of $\beta = \beta_{1MMF}$ (identified as $\beta_0$) rather than $\beta_1$.

## V. SUMMARY AND CONCLUSIONS

The differences between the three approaches to small-signal time- and frequency-response data analysis, designated DSD, CSD0, and CSD1 here, have been discussed and methods described for identifying which one is most appropriate for a given data set and fitting model. A useful table of the limiting low- and high-frequency log–log slopes of response models for all four immittance levels is presented, and an apparent anomaly in the high-frequency $\sigma'(\omega)$ log–log slope for the CSD0 approach is identified and explained. It is shown that the CSD1 temporal relaxation function response is, unlike that for DSD and CSD0 situations, not of the stretched-exponential form when a KWW fitting model is employed.

Detailed fitting results are presented for $Na_2O–3SiO_2$ data at 321 and 380 K in order to illustrate the above differences, justify the choice of a fitting model, and provide material for comparison with the Moynihan modulus formalism fitting approach.

The subtleties in the erroneous interpretations of the widely employed MMF frequency-response data fitting approach have finally been explained after 25 years of use. The matter is complicated because of partly compensating effects and is presented in outline form below.

(a) The MMF is a CSD1 fitting procedure, which not only involves $\epsilon_\infty$ instead of $(\epsilon_{C\infty})_1$, but takes no separate account of the high-frequency-limiting dielectric constant $\epsilon_{D\infty}$ and, thus, leads to incorrect $\beta$ estimates, ones designated $\beta_{1MMF}$ herein.

(b) $\beta_{1MMF}$ has been incorrectly identified in the literature as $\beta_0$, the SE parameter involved in the CSD0 fitting approach. The proper CSD1 fit estimate including $\epsilon_{D\infty}$, $\beta_1$, satisfies $\beta_1 \simeq 1 - \beta_0$ for data well fitted by the KWW model.

(c) Since $\beta_{1MMF}$ values are often found to approximate corresponding $\beta_0$ ones, $1 - \beta_{1MMF}$ should approximate

$\beta_1$ even though the adequacy of the approximation depends on the size of $\epsilon_{D\infty}$.

(d) CSD1 CNLS frequency-response data fitting,[18] using Eq. (4) or (5) and including the effect of $\epsilon_{D\infty}$, should be employed hereafter in place of the MMF approach, and the incorrect Eq. (9) should be replaced by Eq. (7). Previous results obtained using the MMF should be reinterpreted, and even then most of them are likely to be sufficiently approximate that important conclusions should not be based on them.

The first step in gaining insight into the physical processes involved in the dispersive response of a material is obtaining well-determined estimates of the parameters of an appropriate fitting model, including their temperature dependences. Such results should be the foundation of the approach to understanding. But inadequate fitting results, especially when their inadequacy is unrecognized, can lead to the construction of a house of cards, which only supports misleading conclusions.

Even when a best choice of the DSD, CSD0, and CSD1 fitting approaches has been made, one still needs to find and use the best available specific fitting model by comparing fit results with different models. Full complex nonlinear least-squares fitting should be used, with the inclusion in the complete model of electrode polarization effects when needed. The CSD1 approach is the appropriate choice for thermally activated dispersion associated with mobile charges, which can lead to nonzero dc conduction. Although the data for only a few different CSD materials have been analyzed since the recent availability in the LEVM computer program of a KWW algorithm for quick and accurate fitting,[3–5] their results and those herein indicate that the KWW1 model leads to appreciably better fits than others used. Note that the minimum-parameter-number full KWW1 model involves $\rho_{01}$, $\tau_{o1}$, $\beta_1$, and $\epsilon_{D\infty}$.

Since no dispersion model available so far is based on microscopic many-body theory, one must use semiempirical models such as the KWW. Although the KWW temporal response has been derived using a wide variety of physical assumptions, none of such derivations leads to a quantitative understanding of even the temperature dependence of such parameters as the KWW $\beta_0$ and $\beta_1$. Ngai[31] has qualitatively characterized his KWW coupling parameter $n \equiv 1 - \beta_0$ as a measure of the size of ''cooperatively rearranging regions'' of the sample: the larger $n$ and, thus, the larger the size of such entities, the stronger the nonexponential character of the temporal relaxation.

Roland and Ngai[32] and Hodge[33] have also related $n$ (or $\beta_0$) to the fragility of glass-forming liquids, ones which show broader relaxation spectra the greater their fragility. Thus, for decreasing temperature one would expect that $\beta_0$ would decrease and $n$ increase. Although $n$ is intrinsically associated with a temporal response involving $\beta_0$, and $\beta_1$ can, in general, only be obtained, thus far, from the KWW1 frequency-response fitting, to the degree that $\beta_1 \simeq 1 - \beta_0$, $\beta_1$ and $n$ are comparable. Finally, notice that, in the absence of temperature-dependent cutoff effects, while the width of a $-\rho_1''(\omega)$ peak region increases as the temperature increases

and $\beta_1$ decreases, the $-\rho_0''(\omega)$ width of a KWW0 fit decreases as $\beta_0$ increases. It follows that a relation between fragility and the frequency-response spectrum width should most properly involve $\beta_1$.

[1] J. R. Macdonald and J. C. Wang, Solid State Ion. **60**, 319 (1993).
[2] J. R. Macdonald, J. Appl. Phys. **75**, 1059 (1994).
[3] J. R. Macdonald, J. Non-Cryst. Solids **197**, 83 (1996); **204**, 309 (1996); and $G_D$ in Eq. (A2) should be $G_{CD}$, the present $G_{C1}$ quantity.
[4] J. R. Macdonald, J. Non-Cryst. Solids **210**, 70 (1997).
[5] J. R. Macdonald, J. Non-Cryst. Solids **212**, 95 (1997).
[6] P. B. Macedo, C. T. Moynihan, and R. Bose, Phys. Chem. Glasses **13**, 171 (1972); C. T. Moynihan, L. P. Boesch, and N. L. Laberge, Phys. Chem. Glasses **14**, 122 (1973).
[7] *Impedance Spectroscopy—Emphasizing Solid Materials and Systems* edited by J. R. Macdonald (Wiley-Interscience, New York, 1987), p. 96.
[8] S. Havriliak and S. Negami, J. Polym. Sci. **C14**, 99 (1966).
[9] K. S. Cole and R. H. Cole, J. Chem. Phys. **9**, 341 (1941).
[10] D. W. Davidson and R. H. Cole, J. Chem. Phys. **19**, 1484 (1951).
[11] J. R. Macdonald, J. Appl. Phys. **58**, 1955 (1985).
[12] H. K. Patel and S. W. Martin, Phys. Rev. B **45**, 10 292 (1992).
[13] H. Jain and C. H. Hsieh, J. Non-Cryst. Solids **172-174**, 1408 (1994).
[14] K. L. Ngai and A. K. Rizos, Phys. Rev. Lett. **76**, 1296 (1996).
[15] R. Kohlrausch, Pogg. Ann. Phys. Chem. **91**, 179 (1854); G. Williams and D. C. Watts, Trans. Faraday Soc. **66**, 80 (1970); G. Williams, D. C. Watts, S. B. Dev, and A. M. North, *ibid.* **67**, 1323 (1971).
[16] C. P. Lindsey and G. D. Patterson, J. Chem. Phys. **73**, 3348 (1980). The $\rho(\tau)$ function in this work is equivalent to the present $G_D(\tau)$ DRT function.
[17] J. R. Macdonald and M. K. Brachman, Rev. Mod. Phys. **28**, 422 (1956).
[18] J. R. Macdonald and L. D. Potter, Jr., Solid State Ion. **23**, 61 (1987). The new version of the extensive LEVM fitting program, V. 7.01, may be obtained at no cost from Solartron Instruments, Victoria Road, Farnborough, Hampshire, GU147PW, England; electronic mail, attention Mary Cutler, lab_info@solartron.com. More details about the program and how to get it appear in http://www.physics.unc.edu/~macd/
[19] J. R. Macdonald, Solid State Ion. **25**, 271 (1987).
[20] J. R. Macdonald, J. Appl. Phys. **34**, 538 (1963).
[21] K. L. Ngai, Solid State Phys. **9**, 127 (1979).
[22] R. Syed, D. L. Gavin, and C. T. Moynihan, J. Am. Ceram. Soc. **64**, C-118 (1981).
[23] B. A. Boukamp and J. R. Macdonald, Solid State Ion. **74**, 85 (1994).
[24] K. L. Ngai and O. Kanert, Solid State Ion. **53-56**, 936 (1992).
[25] A. S. Nowick and B. S. Lim, J. Non-Cryst. Solids **172-174**, 1389 (1994). I much appreciate the transmittal of these data to me by Professor Nowick.
[26] C. T. Moynihan, J. Non-Cryst. Solids **172-174**, 1395 (1994); **203**, 359 (1996).
[27] I. M. Hodge and C. A. Angell, J. Chem. Phys. **67**, 1647 (1977).
[28] K. L. Ngai and U. Strom, Phys. Rev. B **27**, 6031 (1983).
[29] F. S. Howell, R. A. Bose, P. B. Macedo, and C. T. Moynihan, J. Phys. Chem. **78**, 639 (1974).
[30] C. A. Angell, in *Relaxation in Complex Systems*, edited by K. L. Ngai and G. B. Wright (U.S. Government Printing Office, Washington, DC, 1985), p. 203.
[31] K. L. Ngai, J. Non-Cryst. Solids **131-133**, 80 (1993).
[32] C. M. Roland and K. L. Ngai, J. Non-Cryst. Solids **212**, 74 (1997).
[33] I. M. Hodge, J. Non-Cryst. Solids **212**, 77 (1997).